

# Spectro-photometric characterization of high proper motion sources from WISE

J. C. Beamín,<sup>1,2,3\*</sup> V. D. Ivanov,<sup>1,4</sup> D. Minniti,<sup>5,3,6</sup> R. L. Smart,<sup>7</sup> K. Mužić,<sup>1</sup>  
R. A. Mendez,<sup>8,1,3</sup> Y. Beletsky,<sup>9</sup> A. Bayo,<sup>10,3</sup> M. Gromadzki,<sup>3,10</sup> R. Kurtev,<sup>10,3</sup>

<sup>1</sup>European Southern Observatory, Ave. Alonso de Cordoba 3107, Casilla 19001, Santiago, Chile.

<sup>2</sup>Instituto de Astrofísica, Facultad de Física, Pontificia Universidad Católica de Chile, Casilla 306, Santiago 22, Chile.

<sup>3</sup>Millennium Institute of Astrophysics, Chile.

<sup>4</sup>European Southern Observatory, Karl-Schwarzschild-Str. 2, D-85748 Garching bei München, Germany

<sup>5</sup>Facultad de Ciencias Exactas, Universidad Andres Bello, Fernandez Concha 700, Las Condes, Santiago, Chile

<sup>6</sup>Vatican Observatory, V00120 Vatican City State, Italy

<sup>7</sup>INAF-Osservatorio Astrofisico di Torino, Strada Osservatorio 20, 10025 Pino Torinese, TO, Italy.

<sup>8</sup>Universidad de Chile, Departamento de Astronomía, Casilla 36-D, Santiago, Chile.

<sup>9</sup>Las Campanas Observatory, Carnegie Institution of Washington, Colina el Pino, 601 Casilla, La Serena, Chile

<sup>10</sup>Instituto de Física y Astronomía, Facultad de Ciencias, Universidad de Valparaíso, Ave. Gran Bretaña 1111, Playa Ancha, Valparaíso, Chile.

8 March 2022

## ABSTRACT

The census of the solar neighborhood is almost complete for stars and becoming more complete in the brown dwarf regime. Spectroscopic, photometric and kinematic characterization of nearby objects helps us to understand the local mass function, the binary fraction, and provides new targets for sensitive planet searches. We aim to derive spectral types and spectro-photometric distances of a sample of new high proper motion sources found with the WISE satellite, and obtain parallaxes for those objects that fall within the area observed by the Vista Variables in the Vía Láctea survey (VVV). We used low resolution spectroscopy and template fitting to derive spectral types, multiwavelength photometry to characterize the companion candidates and obtain photometric distances. Multi-epoch imaging from the VVV survey was used to measure the parallaxes and proper motions for three sources. We confirm a new T2 brown dwarf within  $\sim 15$  pc. We derived optical spectral types for twenty four sources, mostly M dwarfs within 50 pc. We addressed the wide binary nature of sixteen objects found by the WISE mission and previously known high proper motion sources. Six of these are probably members of wide binaries, two of those are new, and present evidence against the physical binary nature of two candidate binary stars found in the literature, and eight that we selected as possible binary systems. We discuss a likely microlensing event produced by a nearby low mass star and a galaxy, that is to occur in the following five years.

Key words: astrometry, parallaxes, binaries, brown dwarfs, techniques: spectroscopic.

## 1 INTRODUCTION

High proper motion sources have been studied for over two centuries now, as one might expect that the fastest moving sources would be the closest to our solar system. Since mid XX century, comprehensive searches of high proper motion objects have been performed using photographic plates and later CCD cameras, to find the closest neighbors of the Sun (Giclas et al. 1971; Luyten 1979a,b; Wroblewski & Torres

1989; Hambly et al. 2004; Lépine & Shara 2005; Lépine 2008; Finch et al. 2014, RECONS, among others). However, cool objects are intrinsically faint in the optical and emit most of their light in the near infrared (NIR). Therefore, the searches for unknown nearby sources gradually turn to the NIR wavelengths taking advantage of improved camera sensitivities, spatial and temporal resolution (Deacon et al. 2009; Kirkpatrick et al. 2010; Smith et al. 2014), yielding in the last twenty years the discovery of over two thousand ultra-cool dwarfs. Widening the color space of the searches has helped to improve the stellar and sub-stellar

\* E-mail: jcbeamín@astro.puc.cl

density estimates in the solar neighborhood, and the frequency of low-mass companions, among other questions (Allen et al. 2012; Luhman et al. 2012; Dieterich et al. 2012; Ivanov et al. 2013; Deacon et al. 2014; Davison et al. 2015).

The Wide-field Infrared Survey Explorer (WISE; Wright et al. 2010) satellite has revolutionized the field of brown dwarf with color based selections providing the discovery of hundreds of brown dwarfs (Kirkpatrick et al. 2011). Later, the multiepoch nature of the WISE mission provided proper motions for over twenty thousand individual sources (Luhman 2014; Kirkpatrick et al. 2014), including the discoveries of the third and fourth closest systems to the Sun (Luhman 2013, 2014). These are the closest binary BD, and the coldest BD known. The WISE mission also led to the discovery of the first Y dwarfs (Cushing et al. 2011; Kirkpatrick et al. 2012). Thousands of other interesting objects were found, including young very low mass objects (M, L and T type; Gagné et al. 2015), several ultra cool subdwarfs (Kirkpatrick et al. 2014), etc. These discoveries are helping to better understand the role of temperature, metallicity and evolution in very cool atmospheres. Finally, a new sample of nearby K and M dwarfs ( $d \leq 100$  pc) was created, well suited for exoplanet searches.

Here we report a follow up study of bright high proper motion objects detected by Luhman (2014) and Kirkpatrick et al. (2014), concentrating on objects within 50 pc, wide co-moving binaries, and possible members of nearby young moving groups. The project summarized here was motivated by the recent discoveries of nearby stellar and sub-stellar objects (e.g., Artigau et al. 2010; Lucas et al. 2010; Luhman 2013; Mamajek et al. 2013; Scholz 2014, among others), the implications that these findings may have on the stellar census in the Solar neighborhood (Henry et al. 2006; Faherty et al. 2009; Winters et al. 2015), new results in the multiplicity of young low-mass stars and brown dwarfs in the field and young moving groups (Delorme et al. 2012; Elliott et al. 2014), and even the dynamic interactions of the Solar system (Ivanov et al. 2015; Mamajek et al. 2015). The paper is organized as follows: Section 2 describes the catalogs and methods we used to generate a list of objects of interest, and the instruments we used to follow up and characterize them. In section 3 the methods for classification are presented. Section 4 describes the distance measurements and comparison of photometric and spectroscopic results. Finally, in section 5 we discuss individual sources, and present our conclusions in section 6.

## 2 SAMPLE SELECTION AND OBSERVATIONS

We started by analyzing bright sources in the new catalogs of high proper motion sources by Luhman (2014) and Kirkpatrick et al. (2014). We selected the brightest sources with the highest proper motion that were visible in April from the southern skies (i.e. Dec < 30), with no previous derived spectral types and no data in the ESO archive. We also performed a cross check with previously known high proper motion sources from Simbad (Wenger et al. 2000). If Simbad returned a source within  $15'$  showing a similar proper motion, we selected the brighter one between the SIMBAD match and the WISE object for spectroscopic follow up. We used a relaxed criterion to select candidate companions, i.e. a

Table 1. Sample of WISE high proper motion objects selected for spectroscopic follow up with the EFOSC2 at the NTT at La Silla observatory, and FIRE at Baade at Las Campanas observatory.

Name	R.A.	DEC.	Exposures
2MASS J06571510-1446173	06:57:14.44	-14:46:25.2	2x120
2MASS J07523088-4709470	07:52:31.93	-47:09:49.8	3x60
2MASS J08291581-5850305	08:29:15.28	-58:50:35.2	2x60
2MASS J09432908-0237184	09:43:28.09	-02:37:22.4	3x60
2MASS J10570299-5103351	10:57:01.20	-51:03:37.2	2x120
2MASS J11161471-4403252	11:16:14.91	-44:03:28.4	2x120
2MASS J11163668-4407495	11:16:36.94	-44:07:47.2	3x120
2MASS J13211484-3629180	13:21:13.94	-36:29:11.1	6x120
2MASS J13552455-1843080	13:55:23.50	-18:43:18.1	5x180
2MASS J14033647+0412395	14:03:36.06	+04:12:28.9	5x180
2MASS J14040025-5923551	14:04:00.52	-59:23:53.3	2x120
2MASS J12412819-6507578	12:41:28.10	-65:07:55.6	2x120
2MASS J13322604-6621419	13:32:26.19	-66:21:33.8	3x120
2MASS J14035016-5923426	14:03:50.92	-59:23:45.2	2x120
2MASS J14233830+0138520	14:23:38.27	+01:38:41.7	3x120
2MASS J14574906-3904511	14:57:49.68	-39:04:55.1	5x180
2MASS J15463089-5258367	15:46:31.10	-52:58:32.1	3x60
2MASS J15480441-5810533	15:48:03.58	-58:10:49.9	2x120
2MASS J17345391-6206546	17:34:53.20	-62:06:52.1	3x15
2MASS J19104599-4133407	19:10:45.27	-41:33:46.9	3x120
2MASS J19242108-0804516	19:24:21.09	-08:04:51.6	2x120
2MASS J20044356-7123334	20:04:43.09	-71:23:28.4	2x120
2MASS J21252081-3422144	21:25:20.78	-34:22:20.3	2x120
2MASS J22275385-2337300	22:27:52.75	-23:37:35.1	3x120
WISE J212100.87-623921.6	21:21:00.88	-62:39:21.7	6x63.4

source with proper motion  $\geq 200$  mas yr<sup>-1</sup> and a position angle of proper motion within  $\sim 30^\circ$ . These relaxed constraints caused the selection of some spurious pairs, and we discuss this issue in the coming sections. We also created a reduced proper motion diagram in order to find brown dwarf candidates.

To derive the spectral types of the selected objects, we obtained spectra in the optical and in the near-infrared for WISE J21210032-6239194 (hereafter WISE 2121-6239). In addition, for the objects located within the area covered by the VISTA Variables in the Vía Láctea survey (VVV) we obtained photometry and astrometry.

### 2.1 NTT/EFOSC2

The ESO Faint Object Spectrograph and Camera v.2 (EFOSC2; Buzzoni et al. 1984; Snodgrass et al. 2008) mounted at the 3.6m New Technology Telescope (NTT) at La Silla observatory, is a versatile instrument for low resolution spectroscopy, imaging, and polarimetry. We obtained low resolution long slit spectra for twenty four sources (see Table 1) using the same configuration for all the sources:  $1''$  slit width, grism number one, covering a spectral range of  $\lambda = 3185\text{--}10940 \text{ \AA}$  with a resolution  $\sim 48 \text{ \AA}$ . All the sources were observed on April 17<sup>th</sup> 2014. The usual reduction steps, bias and flat fields corrections were performed, followed by wavelength calibration and flux calibration with the F

<sup>1</sup> According to instrument manual, there is second order contamination for wavelengths longer than  $9280 \text{ \AA}$

type spectro-photometric standard LTT 9239 (Hamuy et al. 1994).

## 2.2 Magellan/FIRE

The Folded-port Infrared Echellette (FIRE; Simcoe et al. 2008, 2010, 2013) mounted at the 6.5m Magellan Baade Telescope uses a 2048×2048 HAWAII-2RG array. It covers the wavelength range from 0.8 to 2.5  $\mu\text{m}$  when used in the high-throughput prism mode, delivering a resolution varying from  $\sim 500$  at  $J$ -band to  $\sim 300$  at  $K$ -band for the  $0''.6$  slit. A spectrum of the objects WISE 2121-6239 was obtained in the ABBAAB pattern, with the exposure time of  $6 \times 63.4$  s. The  $1''$  slit was oriented along the parallactic angle. The read-out mode was “Sample-Up-the-Ramp” (SUTR) with the low gain mode ( $3.8e^-$  per count). The A0V star HD 195288 was observed with the same set up (with the exception of the read out mode, we used mode “Fowler 1” instead) in ABBA pattern, for telluric correction. Low and high voltage (1.5 and 2.5 V) flats were obtained after the observations of the source and the telluric lines to correct the red and blue parts of the spectrum. NeAr lamp spectra were obtained after the observations for wavelength calibration. In addition, we observed an extra lamp with the  $0.45''$  slit to differentiate some blends with lines that help us to improve the wavelength calibration.

The data was reduced with the instrument pipeline `firehose_ld`<sup>2</sup>. It traces the slit, performs a wavelength solution, combines the flat fields and applies them, finding the object on the 2-D image, and finally it extracts a 1-D spectrum.

The individual spectra of the target and the telluric are median-scaled with the `fire_xcombspec` tool and then combined with a Robust Weighted Mean algorithm. Finally, the telluric correction was applied using the `fire_xtellcor_ld`, a clone of the `xtellcor` program from SpexTool (Cushing et al. 2004; Vacca et al. 2003)

## 2.3 VISTA/VIRCAM

The VVV survey (Minniti et al. 2010; Saito et al. 2012; Hempel et al. 2014) is one of the six ESO public surveys carried out with the 4.1m Visual and Infrared Survey Telescope for Astronomy (VISTA) telescope and VIRCAM camera at cerro Paranal Chile (Dalton et al. 2006; Emerson & Sutherland 2010). It has sixteen 2048x2048 pixels chips with a pixel scale of  $0.34''$ . The total field of view is  $\sim 1^\circ \times 1.5^\circ$ . The VVV is a variability survey primarily designed to trace the 3-D structure of the Milky Way, observing  $562^{o2}$  towards the Galactic Bulge and southern inner disk (Gonzalez et al. 2011; Dékány et al. 2013; Minniti et al. 2014). This survey matches the requirements for good estimations of the proper motions (PMs) and parallaxes, as demonstrated previously by Beamin et al. (2013); Ivanov et al. (2013). The data were reduced at the Cambridge Astronomy Survey Unit (CASU) with pipeline v1.3. In this paper we used the astrometric and photometric catalogs generated from individual exposures (named pawprint, see Hempel et al. 2014 for further details), as opposed to catalogs generated from the combined exposures. This way, we

have two independent astrometric/photometric points obtained within a few minutes, where the target is observed by a different detector, giving us a better handling of the systematic uncertainties. We took advantage of the high stellar density of the fields and constructed a local astrometric solution to fit relative proper motion and parallax simultaneously.

## 3 SPECTRO-PHOTOMETRIC CHARACTERIZATION

### 3.1 Spectral typing

Twenty one of the twenty four spectra observed with EFOSC2 showed the characteristic molecular absorption bands M type stars (TiO, CaH), and they were compared to the primary K5V-M9V standards from Kirkpatrick et al. (1991) and Kirkpatrick et al. (1999) available from the Dwarf Archives<sup>3</sup>. The remaining three spectra indicated hotter stars, and for those earlier than K5 type objects we used the standards of Pickles (1998).

The low resolution of our spectra ( $\sim 40 \text{ \AA}$ ) does not allow to use the spectral indexes frequently used in the literature (e.g. Kirkpatrick et al. 1991; Gizis 1997; Lépine et al. 2013) so we relied instead on the overall shape of the spectrum.

The template spectra were smoothed to the resolution of our data, normalized at  $7500 \text{ \AA}$ . To find the best match, we performed a  $\chi^2$  minimization over two different wavelength ranges. First for the twenty later type stars we used the range  $\lambda=6500-9000 \text{ \AA}$ , as most of the flux and spectral features of interest are in that region, also the templates from Kirkpatrick et al. (1991) that we used do not cover bluer wavelengths. For the four hotter objects we minimize over a broader wavelength region,  $\lambda=3500-9500 \text{ \AA}$  as they have more flux towards the bluer regions.

The results are shown in Fig. 1 and 2. The types of some objects were adjusted by up to 0.5 sub-type after a visual inspection.

The derived spectral types are listed in Table 3. We also attempted to fit separately the blue ( $6500-7600 \text{ \AA}$ ) and red ( $7600-9000 \text{ \AA}$ ) parts of each spectrum as shown in Jao et al. (2008) the red part of M sub-dwarfs appears  $\sim 1$  sub-type earlier than their blue part (depending on metallicity). We did not observe this behavior in the previously reported sub-dwarf object 2MASS J14574906-3904511.

The NIR spectra of WISE J2121-6239 was compared to the L and T dwarf spectra from the Spex library<sup>4</sup> using the  $\chi^2$  minimization algorithm, mentioned before, yielding a best match to the T2 type SDSS J175024.01+422237.8. Figure 3 shows the comparison of WISE 2121-6239 against three T sub-types, T1 SDSS J085834.42+325627.7; T2 SDSS J175024.01+422237.8; T3 2MASS J12095613-1004008.

The spectral indexes:  $H_2O-J$ ,  $CH_4-J$ ,  $H_2O-H$ ,  $CH_4-H$  and  $CH_4-K$  from Burgasser et al. (2006) yield a spectral type of  $T2 \pm 1$  (Table 2). Using the tabulated coefficients of Table 14 in Dupuy & Liu (2012) and the 2MASS and WISE

<sup>3</sup> <http://dwarfarchives.org>

<sup>4</sup> <http://pono.ucsd.edu/~adam/browndwarfs/spexprism/library.html>

<sup>2</sup> [http://web.mit.edu/~rsimcoe/www/FIRE/ob\\_data.htm](http://web.mit.edu/~rsimcoe/www/FIRE/ob_data.htm)

Table 2. Main spectral indexes for T dwarfs as given in Burgasser et al. (2006)

Object	H <sub>2</sub> O-J	CH <sub>4</sub> -J	H <sub>2</sub> O-H	CH <sub>4</sub> -H	CH <sub>4</sub> -K	adopted type
WISE J2121-6239	0.55(T2)	0.72(T1)	0.48(T2)	0.93(T1)	0.62(T2)	T2±1

magnitudes we computed a photometric distance between 12-16 pc for this brown dwarf.

### 3.2 SED fitting

We searched various archives for historic multi-wavelength observations of our program targets. Using Aladin (Bonnarel et al. 2000), we were able to retrieve the catalogs and the archival images, for visual inspection to ensure that our high PM target cross identifications were correct. We also used Topcat (Taylor 2005) to cross-match catalogs.

To build the SED and compare to stellar models we used the Virtual Observatory SED analyzer (VOSA; Bayo et al. 2008), fitting the BT-settl models 2012 (Allard et al. 2012) to the data, first with a Bayesian approach, and then constraining the model parameters with a  $\chi^2$  minimization over a three parameter space: effective temperature  $T_{eff}$ , surface gravity  $logg$ , and metallicity [Fe/H]. Increasing the number of photometric measurements and widening the wavelength coverage makes the fit more robust and reliable.

The  $T_{eff}$  is the most stringently constrained parameter, with uncertainties of order of  $\sim 200$  K. The other parameters  $logg$  and [Fe/H], were not well constrained and usually presented flat probabilities distribution in the Bayes analysis. Nevertheless, all the sources were fitted with  $logg \geq 4$ , and  $[Fe/H] \geq -1$ , the only exception was 2MASS J15463089-5258367, which was better fitted with lower metallicity values ( $-2 \leq [Fe/H] \leq -1.5$ ). The photometry used in the SED fit is available in the online version of Table 3.

In order to use the optical catalogs GSC2.3, USNO-B1, UCAC4 and CMC15 (Lasker et al. 2008; Monet et al. 2003; Zacharias et al. 2013; Muñoz & Evans 2014), we had to make the following assumptions: The first and second Blue/Red photographic band from GSC2.3 were used as Johnson B/R bands (when two epochs were available for a given band we use the mean). For USNO-B1 we used  $B_j$  as Johnson B band and V mag as Johnson V. For UCAC4 catalog, when the source had only R band measurement, we used the UCAC R filter from VOSA, but, in the last release of UCAC4, they do not list the R magnitude, they transformed the old optical magnitudes to Johnson B and V and to Sloan r, i filters, and we adopted those values and filter systems. For these three catalogs we assigned a photometric error of 0.3 mag. CMC15 uses the SDSS r filter, the difference with the Sloan r system is of the order of 0.02mag, and a typical error of 0.08 mag at magnitude  $r \sim 16$  is listed in the documentation file<sup>5</sup>. To be safe we assumed a fixed value of 0.1 mag for the error in the photometry.

We performed several simulations letting the uncertainties of USNO-B1, GSC2.3 and UCAC4, vary between 0.2 and 0.5 mag, and removing some of the photometric points to

see how much do these assumptions affect the final fit. The SED parameter change within the uncertainties listed above  $\Delta T_{eff} \sim 100$  K,  $\Delta logg \sim 0.5$ ,  $\Delta [Fe/H] \sim 0.5$ .

In Table 4 we provide the object 2MASS name, spectral type from our EFOSC2 spectra and the uncertainty, and the effective temperatures obtained through SED fit using VOSA and archival photometry, using the BT-Settl models ( $log g$  and metallicities were free parameters and were almost always above 4.5 and -1, respectively)<sup>6</sup>

To compare the spectral and the SED results we converted the spectral types into effective temperatures using the relations of Pecaut & Mamajek (2013)<sup>7</sup>. We found a typical agreement within  $\sim 100$  K between the two methods.

## 4 DISTANCE ESTIMATION

### 4.1 Spectro-photometric distances

We estimated the distances to the objects and their companions from the derived spectral types and  $T_{eff}$  from the 2MASS  $J$  and  $K_S$  photometry using the absolute magnitudes from Pecaut & Mamajek (2013). For each object we calculated the distances for the two bands separately. The mean difference is  $3.1\% \pm 1.7\%$ , with a maximum value of 5.6% for object 2MASS J1403+0412. Our final estimate was the average of the two measurements. The sub-type error classification affects the distance estimation by a factor of 15%, on average. The photometric uncertainties introduce errors within 1-3% in the magnitude range we examine. Therefore, estimated spectro-photometric distances will have an associated error of  $\lesssim 20\%$ , of the same order as the differences between our measurements and the values available in the literature (Table 4). A comparison between the values for the distances in the literature and the values we obtain in this study is shown in Fig. 4. The error bars correspond to 15% of their distances in each axis. The only exception is 2MASS J1546-5258, as this source has three distances estimates in the literature, We plotted the average value of the distance and quote the standard deviation around the mean as the error.

### 4.2 Parallax distances

Four objects in our list lie within the VVV survey footprint: 2MASS J14035016-5923426, 2MASS J14040025-5923551, 2MASS J15464497-5254371, 2MASS J15463089-5258367,

<sup>6</sup> The only two objects that were automatically fitted by lower metallicities, 2MASS J1457-3904 and 2MASS J15463089-5258367, are a known sub-dwarf and a early K star.

<sup>7</sup> We used the table version 2014.09.29, available at [http://www.pas.rochester.edu/~emamajek/EEM\\_dwarf\\_UBVIJHK\\_colors\\_Teff.txt](http://www.pas.rochester.edu/~emamajek/EEM_dwarf_UBVIJHK_colors_Teff.txt)

<sup>5</sup> [http://svo2.cab.inta-csic.es/vocats/cmc15/docs/CMC15\\_Documentation.pdf](http://svo2.cab.inta-csic.es/vocats/cmc15/docs/CMC15_Documentation.pdf)

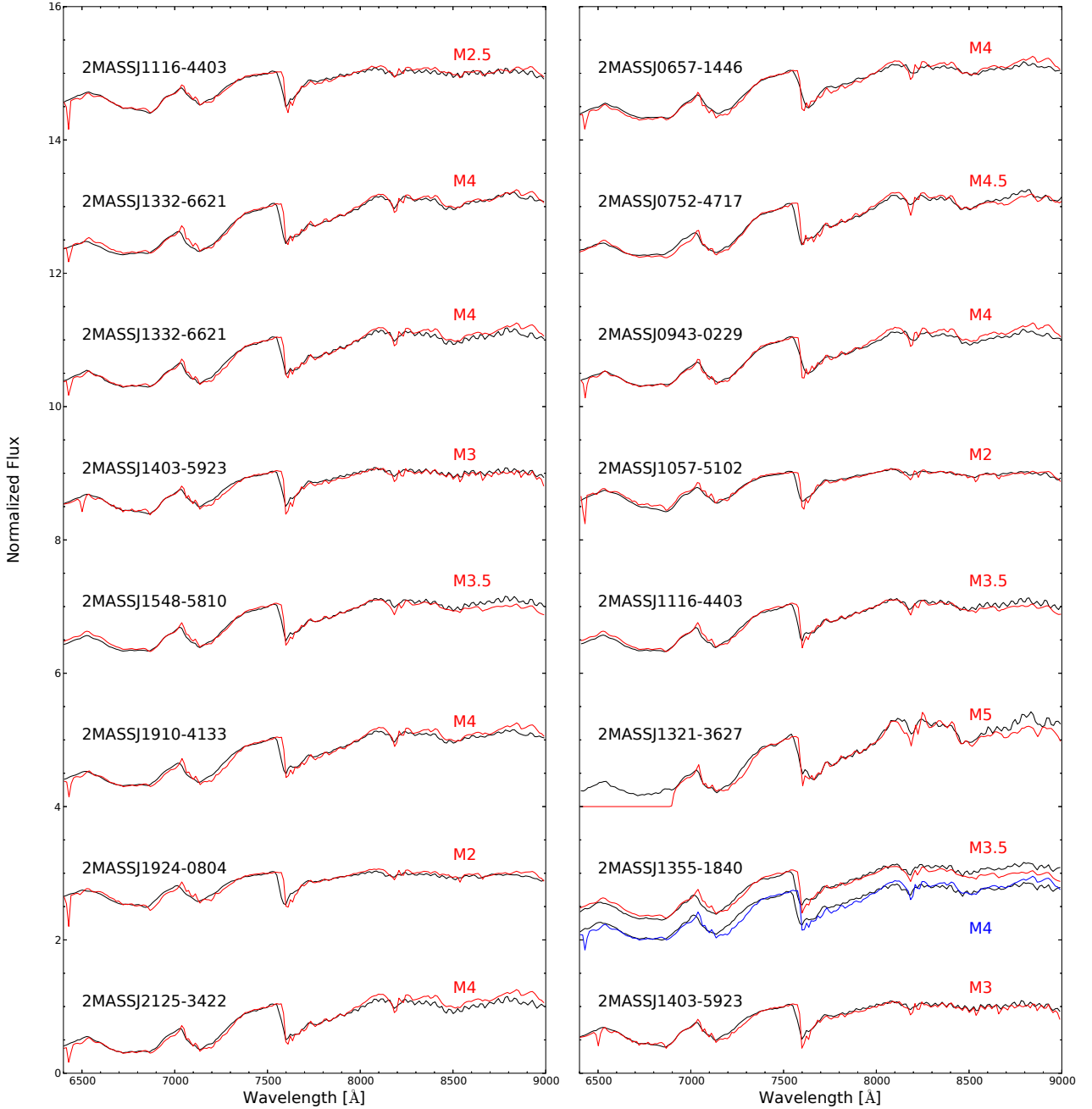


Figure 1. Each panel show the best  $\chi^2$  fit to the spectrum from the set of spectral templates given in Table 4, the templates spectra are taken from the primary standards from Kirkpatrick et al. (1991). In the case of 2MASS 1355-1840 we over-plotted the two best fits, as they fit slightly better different wavelength regions.

but the last one is badly saturated in  $K_S$ , and reliable positions could not be determined. Therefore, we measure the parallaxes only for the first three sources using the procedure developed in the Torino Observatory Parallax Program described in Smart et al. (2003). This has been adapted to the format of the VVV data products (coordinates and photometry) delivered by CASU<sup>8</sup>. A detailed description of

the parallax code can be found in that paper, and we give here only a brief description of the steps involved. For the purpose of the astrometric reduction, we selected reference stars in a circle of radius  $1'$  around the target which, given the high stellar density in these fields, provides an adequate number of reference stars (above a hundred sources). These were selected among the highest S/N objects in the field of view, satisfying the condition that they appear in at least 80% of the frames, and do not exhibit large proper-motions.

For example, for 2MASS 15464497-5254371 the initial number of reference stars was 189, but in the end only 121

<sup>8</sup> <http://casu.ast.cam.ac.uk/surveys-projects/vista/data-processing>

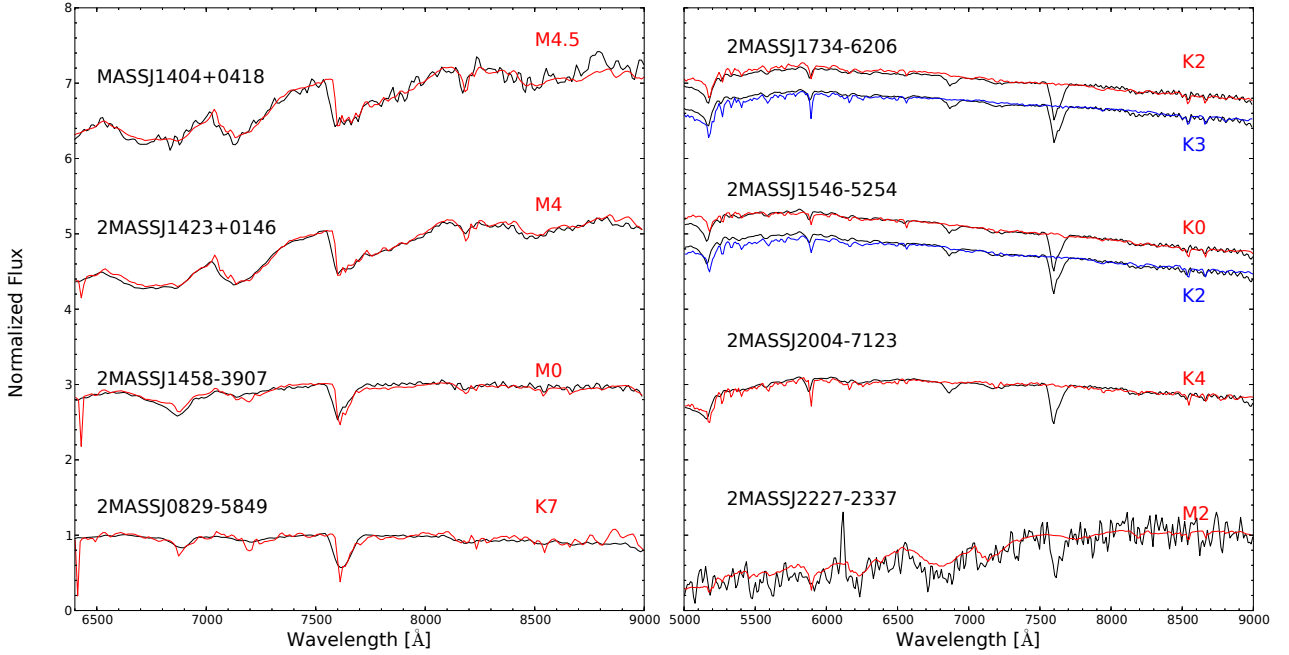


Figure 2. Left panel same as Fig 1. Right panel show the earlier type objects, as the Kirkpatrick et al. (1991) only goes until K5 we used templates from Pickles (1998). For object 2MASS 1546-5252 we assume a K1 spectral type, a compromise between the fit to the continuum of a K0 standard and the Mg absorption around 5170Å of the K2 standard.

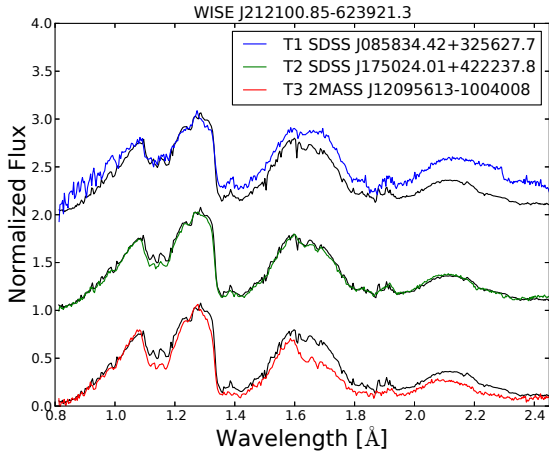


Figure 3. Black spectrum shows the new T2 dwarf WISE 2121-6239 compared to T1 template Burgasser et al. (2010) T2 and T3 template Burgasser et al. (2004).

of these were used to build the astrometric reference frame. In total we had 70 VVV images in  $K_s$ , at various epochs (see Figure 5), spanning more than 3 years. Four epochs were excluded from the solution due to their high residuals with respect to the mean solution. Despite the relatively small parallax, the long baseline and the parallax factor coverage provide a small final error of 1.80 mas. The conversion from relative to absolute parallax, which in any case is quite small (less than 0.4 mas), was computed using the Galactic model by Mendez & van Altena (1996), extended to IR-wavelengths. The proper motion and parallaxes for

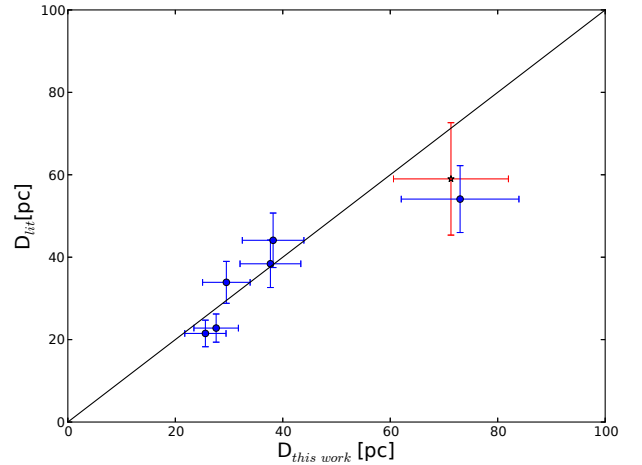


Figure 4. Literature photometric distances v/s spectro-photometric distances from this work for objects within 100 pc. The red star represents the average of the three distance from the literature for source 2MASS J1546-5258, and the error in the Y axis for this source is the dispersion around the mean. The solid black line shows a 1:1 relation, and not a fit to the data points.

these three sources are listed in Table 4, and Fig. 5 show the observations of each source and the best fits.

The binary system 2MASS J14035016-5923426 and 2MASS J14040025-5923551 was on the border of two adjacent chips in the observational sequence and both objects are very bright often saturating in good seeing. This led to high centroiding errors and a sparse reference star set of only 41 and 55 objects for the two fields respectively. The two parallax solutions were therefore completely independent with

Table 3. Archival photometry for sources selected for EFOSC2 spectroscopy and candidate companions

Column name	Description.
2MASS	Name from 2MASS point source catalog
Spectra	Spectroscopy available for this object
B	B from GSC2.3 or USNO-B1
V	V from GSC2.3 or USNO-B1
R	R from GSC2.3 or USNO-B1
I	I from Super Cosmos $I_{IVN}$
RUCAC	old R from UCAC4
J <sub>2MASS</sub>	2MASS J
e_J <sub>2MASS</sub>	Error in J <sub>2MASS</sub>
H <sub>2MASS</sub>	2MASS H
e_H <sub>2MASS</sub>	Error in H <sub>2MASS</sub>
K <sub>S2MASS</sub>	2MASS K <sub>S</sub>
e_K <sub>S2MASS</sub>	Error in K <sub>S2MASS</sub>
W1	WISE W1
e_W1	Error in W1
W2	WISE W2
e_W2	Error in W2
W3	WISE W3
e_W3	Error in W3
W4	WISE W4
e_W4	Error in W4
I <sub>DENIS</sub>	DENIS I
e_I <sub>DENIS</sub>	Error in I <sub>DENIS</sub>
J <sub>DENIS</sub>	DENIS J
e_J <sub>DENIS</sub>	Error in J <sub>DENIS</sub>
K <sub>S DENIS</sub>	DENIS K <sub>S</sub>
e_K <sub>S DENIS</sub>	Error in K <sub>S DENIS</sub>
u <sub>SDSS</sub>	SDSS u
e_u <sub>SDSS</sub>	Error in u <sub>SDSS</sub>
g <sub>SDSS</sub>	SDSS g
e_g <sub>SDSS</sub>	Error in g <sub>SDSS</sub>
r <sub>SDSS</sub>	SDSS r or new UCAC4 r * or CMC15 r **
e_r <sub>SDSS</sub>	Error in r <sub>SDSS</sub>
i <sub>SDSS</sub>	SDSS i or new UCAC4 i *
e_i <sub>SDSS</sub>	Error in i <sub>SDSS</sub>
z <sub>SDSS</sub>	SDSS z
e_z <sub>SDSS</sub>	Error in z <sub>SDSS</sub>
Y <sub>UKIDSS</sub>	UKIDSS Y
e_Y <sub>UKIDSS</sub>	Error in Y <sub>UKIDSS</sub>
J <sub>UKIDSS</sub>	UKIDSS J
e_J <sub>UKIDSS</sub>	Error in J <sub>UKIDSS</sub>
H <sub>UKIDSS</sub>	UKIDSS H
e_H <sub>UKIDSS</sub>	Error in H <sub>UKIDSS</sub>
K <sub>UKIDSS</sub>	UKIDSS K
e_K <sub>UKIDSS</sub>	Error in K <sub>UKIDSS</sub>
Z <sub>VVV</sub>	VVV Z
e_Z <sub>VVV</sub>	Error in Z <sub>VVV</sub>
Y <sub>VVV</sub>	VVV Y
e_Y <sub>VVV</sub>	Error in Y <sub>VVV</sub>
J <sub>VVV</sub>	VVV J
e_J <sub>VVV</sub>	Error in J <sub>VVV</sub>
H <sub>VVV</sub>	VVV H
e_H <sub>VVV</sub>	Error in H <sub>VVV</sub>
K <sub>S VVV</sub>	VVV K <sub>S</sub>
e_K <sub>S VVV</sub>	Error in K <sub>S VVV</sub>

SDSS (DR9), GSC2.3, USNO-B1, UCAC4, CMC15, DENIS, VVV (DR3), 2MASS, WISE (Ahn et al. 2012; Lasker et al. 2008; Monet et al. 2003; Zacharias et al. 2013; Epchtein et al. 1997; Hempel et al. 2014; Skrutskie et al. 2006; Wright et al. 2010).

\* Magnitudes from UCAC4 transformed to SDSS r and i filters, we assume a fixed error of 0.3 mag.

\*\* Magnitudes from CMC15, the catalog mentions they use a SDSS r filter, we assumed 0.1 errors (see discussion of errors in the text). This table is available in a machine-readable form in the online journal. Headers and description of the columns are shown here for guidance only.

different reference fields and with observations from different VIRCAM chips.

Each observation has a quote positional error from the VISTA pipeline but there is a significant fraction of the total that is systematic in nature from transforming the observations to a common system. For this reason when calculating the errors of the derived parallax we do not use the individual observation errors. The final quote errors on the target parameters are obtained from the covariance matrix of the solution scaled by the error of unit weight.

The observations used in the sequence are selected using the standard outlier rejection criteria developed in the Torino program following these two criteria: 1) the average per coordinate error of the reference stars in a frame must be less than the mean error of all frames plus three standard deviations about the mean; 2) The combined observed-minus-computed coordinate residual of each observation must be less than three times the sigma of the whole solution. The objects 2MASS J15464497-5254371, 2MASS J14035016-5923426 and 2MASS J14040025-5923551 had 4, 2 and 2 observations rejected respectively by these criteria.

Extensive bootstrap-like testing was carried out on the observations to make sure the results were robust. This consisted of iterating through each observation and using as the primary base frame and thus making a solution that that incorporated slightly different sets of reference stars and a different starting point within the sequence. The solution chosen for publication is that one which is closest to the median of all solutions. The majority of the solutions (>90%) were all within one sigma of the chosen solution.

## 5 DISCUSSION AND REMARKS ON INDIVIDUAL OBJECTS

We determined physical properties and distances for twenty five stars, most of which are within  $D \sim 140$  pc from the Sun. Only eight of these had previously determined distances. Thirteen of the stars are located within  $D \sim 50$  pc. Given that our selection of targets from the WISE high PM list was not systematic, and that the list itself is not a complete census of the objects within  $D \sim 50$  pc we did not attempt to do a completeness analysis. The derived spectral types range from early-K to mid-M.

The high transverse velocities of 2MASS J173453.91-620654.6, 2MASS J140336.47+041239.5 and 2MASS J145749.06-390451.1 and the co-moving binary pair 2MASS J08291581-5850305 (or L 186-122) and 2MASS J08292286-5849209, make them likely members of the Galactic halo. The remaining objects probably belong to the disc population.

### 5.1 Probable multiple systems

We adopted binarity criteria requiring: common PMs i.e.  $\Delta\theta\Delta\mu \leq (\mu/0.15)^{3.8}$ , where  $\Delta\theta$  and  $\Delta\mu$  are the angular separation (in arcseconds) and the difference in the magnitude of the proper motion vectors (in arcseconds per year) (See Sect. 2.2. in Lépine & Bongiorno 2007), distances in agreement at the  $2\sigma$  confidence level, and consistency between the spectral types and the apparent magnitudes.

Table 4. Spectral classification and spectro-photometric distances for the stars observed with EFOSC2@NTT.

2MASS Name	Sp. type	SED $T_{eff}$	J	$\mu_{\alpha}\cos(\delta)$ [mas]	$\mu_{\delta}$ [mas]	d[pc] (lit.)	d[pc](this work)	ref.
J06571510-1446173	M4 $\pm 0.5$	3300	10.678	70	-270	–	29.1	this work <sup>a</sup>
J07523088-4709470	M4.5 $\pm 0.5$	3200	11.738	-109	176	44.1 <sup>b</sup>	38.2	4
J08291581-5850305	K7 $\pm 1$	4200	10.206	382	-74	–	80.3	5
J09432908-0237184	M4 $\pm 0.5$	3200	10.869	-200	-95	–	31.0	4
J10570299-5103351	M2 $\pm 0.5$	3500	11.155	-617	78	54.1	73.0	6
J11161471-4403252	M2.5 $\pm 0.5$	3600	10.649	-492	-3	–	52.2	1
J11163668-4407495	M3.5 $\pm 0.5$	3300	9.917	-518	-29	21.5 <sup>b</sup>	25.6	2
J12412819-6507578	M4 $\pm 0.5$	3100	10.526	-499	-081	–	26.2	1
J13211484-3629180	M5 $\pm 0.5$	2900	12.136	-513	-209	38.4	37.7	6
J13322604-6621419	M4 $\pm 0.5$	3200	10.826	-294	226	–	31.4	1
J13552455-1843080	M4 $\pm 0.5$	3200	14.042	-317	-96	–	136.1	3
J14033647+0412395	M4.5 $\pm 1$	3000	15.853	-233	-073	–	250.3	7
J14035016-5923426	M3 $\pm 0.5$	3500	10.258	11.5 $\pm$ 5.1	-492.2 $\pm$ 4.3	–	20.4 $^{+3.4}_{-2.6}$	this work
J14040025-5923551	M2.5 $\pm 0.5$	3600	10.219	8.3 $\pm$ 5.9	-494.5 $\pm$ 5.1	–	24.8 $^{+5.4}_{-3.7}$	this work
J14233830+0138520	M4 $\pm 1$	3000	12.374	-221	-195	–	52.8	7
J14574906-3904511	M0 $\pm 1$	3900	13.693	-121	-405	215.6	328.6	6
J15463089-5258367	K1 $\pm 1$	4700	8.737	-217	-199	44 <sup>b</sup> ;77 <sup>b</sup> ;56 <sup>b</sup>	71.3	8,9,10
J15464497-5254371	–	3100	12.340	-296.6 $\pm$ 0.8	-109.8 $\pm$ 0.9	–	42.6 $^{+3.6}_{-3.0}$	this work
J15480441-5810533	M3.5 $\pm 0.5$	3400	10.169	-503	-207	33.9 <sup>c</sup>	29.5	1,10
J17345391-6206546	K3 $\pm 1$	4800	10.364	-203	-390	–	131.5	1
J19104599-4133407	M4 $\pm 0.5$	3300	10.610	68	-735	22.8 <sup>d</sup>	27.6	2
J19242108-0804516	M2 $\pm 0.5$	3700	10.766	-196	-379	–	59.8	1
J20044356-7123334	K4 $\pm 1$	4500	10.168	80	-360	–	108.2	3
J21252081-3422144	M4 $\pm 0.5$	3300	10.895	-35	-450	–	32.3	1
J22275385-2337300	M2 $\pm 1$	3600	14.422	-62	-176	–	322.0	3

The Photometric distance error from this work are  $\lesssim 20\%$ . <sup>a</sup>: we recalculated the proper motion using 2MASS and the WISE ALL-SKY epoch position with the highest S/N, as we find that the [Salim & Gould \(2003\)](#) value for proper motion of LP 721-15 is inconsistent with the motion of the sources in the images, this object could be an unresolved binary, and then located further away, see text for discussion; <sup>b</sup>: photometric distance (spectral type derived from  $T_{eff}$  using the relations in [Pecaut & Mamajek \(2013\)](#) and on-line table maintained by E. Mamajek, see text for the link); <sup>c</sup>: parallax distance; <sup>d</sup>: the paper cites the value for other object of the system (SIPS 1910-4133A) and is from photographic plates, our measurement is for SIPS 1910-4133B. The values of proper motion and distances with quoted errors were fitted from VVV data: (1) [Luhman \(2014\)](#); (2) [Winters et al. \(2015\)](#); (3) [Salim & Gould \(2003\)](#); (4) [Finch et al. \(2007\)](#); (5) [Luyten & Hughes \(1980\)](#); (6) [Subasavage et al. \(2005\)](#); (7) [Lépine & Shara \(2005\)](#); (8) [Ammons et al. \(2006\)](#) (9) [Fresneau et al. \(2007\)](#); (10) [Pickles & Depagne \(2010\)](#)

Based on these criteria we identify six probable multiple system, five previously reported systems, and discovering one new one. The following stars are most likely real gravitationally bound systems:

- 2MASS J06571510-1446173 (or LP 721-15) and 2MASS J06571773-1446382;
- 2MASS J08291581-5850305 (or L 186-122) and 2MASS J08292286-5849209;
- 2MASS J14040025-5923551 (or L 197-165) and 2MASS J14035016-5923426;
- 2MASS J15480325-5811119 (or LHS 3119) and 2MASS J15480441-5810533;
- 2MASS 19103460-4133443 (or SIPS1910-4133A), 2MASS 19104599-4133407 (or SIPS1910-4133B) and 2MASS 19103359-4132505 (or SIPS1910-4132C);
- 2MASS J20044356-7123334 (or LTT 7914) and 2MASS J20043661-7123532.

Their parameters are listed in Table 5.

The triple system 2MASS 19103460-4133443, 2MASS 19104599-4133407 B and 2MASS 19103359-4132505 C was reported by ([Lépine 2005](#); [Deacon et al. 2005](#); [Hambly & Deacon 2005](#)). The last work discussed the possibility that this is actually a quadruple system because the magnitude of the component B is  $\sim 0.5$  mag brighter than

the C component. The spectro-photometric and SED based distances all agree within the  $1\sigma$  errors (see Table 5. When we compare the  $T_{eff}$  obtained via SED fit of components B and C we find a difference of  $\sim 200$  K which would be sufficient to explain the 0.5 mag difference (that difference can be less given the error bars for temperature estimates). But we think that is not necessary to invoke a possible equal mass unresolved binary in component B to explain that difference in magnitude, and it is more likely to be explained as an effect of slight difference ( $\sim 100$ -200 K) in  $T_{eff}$ .

2MASS J14040025-5923551 and 2MASS J14035016-5923426 are co-moving. Our spectra suggest this is a M3+M2.5 nearly equal mass binary. Despite the saturation, we were able to measure a parallax from the multi-epoch VVV data:  $40.35 \pm 7.19$  mas and  $49.07 \pm 7.06$  mas ( $24.78^{+5.4}_{-3.7}$  pc and  $20.4^{+3.4}_{-2.6}$  pc) respectively.

2MASS J20044356-7123334 (or LTT 7914) was observed by the RAAdial Velocity Experiment (RAVE) in its fourth data release [Kordopatis et al. \(2013\)](#) and described there. They derived a  $T_{eff}=4817$  and  $\log g=4$  and metallicity  $[\text{Fe}/\text{H}]=0.05$ , based on this we could assume the dwarf nature and apply the relations described before, deriving a distance of 108 pc. They also obtained a radial velocity of  $RV_{\text{Heliocentric}}=-50.2 \pm 2.2$  km s<sup>-1</sup> Our best spectral type for this object is K2, the reference  $T_{eff}$  for a

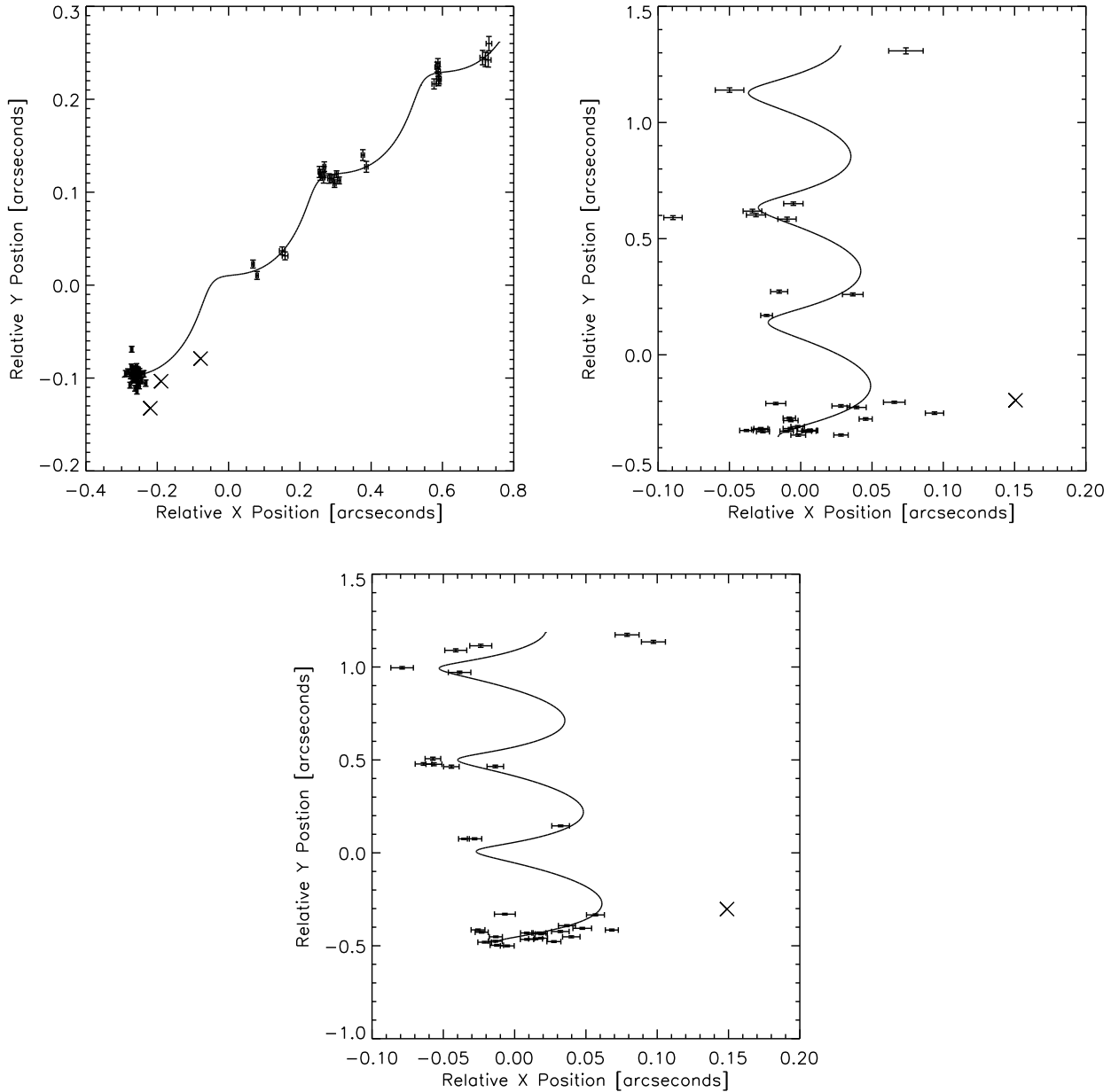


Figure 5. Relative displacement of the targets 2MASS 15464497-5254371, 2MASS J14040025-5923551 and 2MASS J14035016-5923426 with respect to the adopted reference frame as a function of time (top of each plot epoch 2010, bottom of each plot, epoch 2013). A base-frame was chosen for the registration of all other frames to account for small offsets and rotation between them. The fitted parallax wobble, shown by the solid line, is clearly seen in the observations which are plotted as crossed error bars representing the formal VISTA pipeline errors. Any rejected observations within the plot ranges are plotted as Xs.

K2V star is  $\sim 5000$  K so our classification might be revised by one sub-type. Applying photometric SED fitting we obtained a  $T_{eff}=4500$  K  $\pm 100$ ,  $\log g=5 \pm 1$  and metallicity  $[Fe/H]=0.3 \pm 0.5$ . The photometric spectral type would be K4, which is 2 spectral types later than the fit from our optical spectroscopy and one later than the type inferred by RAVE. For a range of photometric distances for K2-K4 types we obtain distances of 100-130 pc, implying a tangential velocity of 170-225  $\text{km s}^{-1}$ , typical for thick disk or halo objects. Interestingly, the available data does not support a low metallicity for this object. For the co-

moving star 2MASS J20043661-7123532 the best photometric fit was  $T_{eff}=3100$  K  $\pm 100$ ,  $\log g=5.5 \pm 1$  and metallicity  $[Fe/H]=-1 \pm 0.5$ . Assuming a spectral type of M4-M5, the distance would be 80-120 pc in agreement within the errors to the estimated value for 2MASS J20044356-7123334. The objects are separated by  $38.7''$  on the sky, which corresponds to  $\sim 4200$  AU for a distance of 110 pc.

Object 2MASS J22275385-2337300 (or LP 876-22) was observed by mistake, as the real new binary candidate was LP 876-1 and 2MASS J22274199-2337283. The observed target was classified as M2  $\pm 1$  star, if we compute the distance

we obtain 322 pc which will put this object in a tangential velocity over 250 km/s and hence probably this object belongs to the halo population, but the distance might be considerably less if we consider that this object might be metal poor, as happened to be with previous sources. We perform the SED fitting to the co-moving pair LP 876-1, 2MASS J22274199-2337283 and they were classified as a M3.5-M8.5, that would imply a distance between 40 pc-50 pc, but further observations are required to settle their true nature.

## 5.2 Rejected multiple systems

The following objects are not real physical pairs, the argument for rejecting them as binaries are: the total proper motion, position angle of motion, spectral types compared to photometric spectral type and distances estimates for the primary and secondary, do not agree within the expected errors.

- 2MASS J07523088-4709470 and 2MASS J07523777-4717270;
- 2MASS J09432908-0237184 and 2MASS J09434389-0229570;
- 2MASS J10570299-5103351 and 2MASS J10573037-5102190;
- 2MASS J11163668-4407495 (or LHS 2386) and 2MASS J11161471-4403252 (see text);
- 2MASS J13211484-3629180 and 2MASS J13214404-3627316;
- 2MASS J13552455-1843080 (or LP 799-1) and 2MASS J13553933-1840586;
- 2MASS J14033647+0412395 and 2MASS J14040651+0418532;
- 2MASS J14233830+0138520 and 2MASS J14234208+0146235;
- 2MASS J14574906-3904511 and 2MASS J14582414-3907504;
- 2MASS J15463089-5258367 and 2MASS J15464497-5254371.

2MASS J07523088-4709470 and 2MASS J07523777-4717270: The second object moves  $\sim 2$  times faster than the first object ( $>5\sigma$  outlier) and the derived  $T_{eff}$  of the secondary (the fainter source) is 200 K higher. Given the classification of M4.5V for the primary, this would place the secondary at least twice as far.

2MASS J11163668-4407495 (or LHS 2386) and 2MASS J11161471-4403252 these were classified and found to be a co-moving pair observed by G.P. Kuiper and re-classified in [Bidelman \(1985\)](#), he classified LHS 2386 as M3: We obtain a best fit with M3.5V and M2.5 for 2MASS J11161471-4403252. [Luhman & Sheppard \(2014\)](#) list these sources as a co-moving binary, because the difference in total proper motion and position angle is small (4.5% and 1.6% respectively). Also the probability of being a chance alignment is below 10% based on the criteria from [Lépine & Bongiorno \(2007\)](#). However, the distance we derive for the two stars are only consistent at  $3\sigma$  level. We obtain half the distance for LHS 2386 than for 2MASS J11161471-4403252. Even if 2MASS J11161471-4403252 is an equal mass binary that would place it around 44-50 pc  $\sim 10$ -15 pc farther away than we expect for LHS 2386. In this hypothetical case, the distances will agree within the errors, that would mean that

at  $5.9'$  of angular separation and distances between 44 and 50 pc, the projected physical separation would be  $\sim 15$ -20 thousand AU which would place them as one of the scarce population of very low mass and very wide binaries within 50 pc. Radial velocities of both stars and a more robust estimation of their distances are needed to disentangle their true nature, but we do not list it as a physical pair with the present evidence.

2MASS J14574906-3904511 and 2MASS J14582414-3907504 have PMs that agree within 1% when comparing the 2MASS and WISE positions, and the position angle of the motion differ only by one degree, these stars should probably be a real physical pair. On the other hand the inferred spectro-photometric distance for the primary is 328.7 pc, while for the secondary using the SED fit we obtain a distance around 40 pc for spectral type M7. In [Jao et al. \(2008\)](#) they found that the primary object is actually a MI.0VI subdwarf and the distance derived by [Subasavage et al. \(2005\)](#) is 215.6 pc even assuming this shorter distance the object is not consistent with a real binary and would imply a high tangential velocity of 432 km/s. Finally, the angular separation of  $445.9''$  means that the projected physical separation at 215.6 pc would be 0.466 pc. Combining these two arguments we argue this is not a real binary.

2MASS J15463089-5258367 and 2MASS J15464497-5254371 [Ammons et al. \(2006\)](#) derived a distance  $44^{+30}_{-15}$  pc and estimated a  $T_{eff}=4669$ -4754 K (according to different fitting functions) based on Hipparcos (Tycho) data for the first object. Other two attempts to measure the distance from photometry are available from [Fresneau et al. \(2007\)](#) and [Pickles & Depagne \(2010\)](#) they obtained 56 pc (no error bars) and  $77^{+50}_{-22}$  pc respectively. Our best SED fit yields 4700 K, in agreement with [Ammons et al. \(2006\)](#), but our best spectrum fit is between K0V-K2V. If we assume this as the correct spectral type, then the photometric distance we obtain is between 68-77 pc, for K0-K2 respectively. For the second object we were able to derive a distance based on parallax from VVV, as discussed in the previous section  $\pi=23.5\pm 1.8$  mas ( $42.6^{+3.6}_{-3.0}$  pc). The parallax and proper motion of 2MASS J15464497-5254371 are shown in Figure 5 and Table 4. The distance agrees very well with the value derived by [Ammons et al. \(2006\)](#), but is almost  $3\sigma$  away from the photometric distance to 2MASS J15463089-5258367, in addition to the difference in the proper motion between the primary (from Tycho-2 catalog [Høg et al. 2000](#)) and our measurements for the candidate companion are too large. The evidence does not support that these two stars form a real binary, the parallax and more accurate proper motions for both sources will be measured by Gaia mission, and then the true nature of these objects will be settled.

## 5.3 Possible future microlensing event

While looking for the available photometry for the object NLTT 37178 from the virtual observatory, we found a nearby source, classified as extragalactic (photometric redshift 0.13) with photometry from SDSS and GALEX. In the following years this object will be getting closer until the closest approach to the center, with the closest approach of  $0.6''$  in 4-8 years. Some extended emission in the galaxy is visible on SDSS images, and we can expect that the nearby star can act as a lens for the outskirts of this galaxy. Deep U and

B band pre-lensing observations are needed to characterize the background source. Search for microlensing events during the next few years may be promising. The most favorable filters to observe the galaxy will be U,B (and/or UV filters from space). The microlensing event might help to understand the real nature and physical properties of this object, e.g. if it is an unresolved binary or hosts a planet. More robust distance estimations (parallax) are necessary, to better constrain the Einstein radius for the system. We assumed a mass of  $0.2M_{\odot}$  for the lens and distances of 40 pc and 543.9 Mpc (co-moving radial distance<sup>9</sup>) for lens and source respectively, and obtain a crude estimate of the Einstein radius of 6.4 mas. As the lensed source is resolved, we might expect variations on the light curve due to lens magnifying different parts of the galaxy.

## 6 CONCLUSIONS

We performed spectroscopic follow up for over twenty new high proper motion objects found by the WISE satellite, and looked for possible new wide binary companions. We found one T2 dwarf probably located within 15 pc. We obtained optical spectral types and photometric distances for 24 objects, as well as parallax measurements for 3 of them. We present some additional evidence for six co-moving objects that are likely physical pairs, two of them are new binary candidates. Four objects are probable members of the galactic halo given their large tangential velocities.

Most of the objects analyzed in this study are located within 75 pc from the Sun, and are bright enough for further follow up and search for planets using state of the art and upcoming NIR instruments.

The use of relatively loose constraints when selecting possible wide co-moving companions given the inhomogeneity of resources available in the literature prove useful to find new co-moving stars. This causes many false positives, but they can be eliminated a posteriori using multiple arguments, combining proper motion, physical separation and spectral energy distributions in the calculation of photometric distances. It is also important to emphasize the relevance of obtaining distances or spectral types for discriminating chance alignments from real wide binaries (or co-moving stars), even when the proper motion and position probabilities are very low we show two examples in this paper where the hypothesized binaries are most likely not physically related.

We also discussed a likely microlensing event due to a star passing in front of a background galaxy. The number of predicted microlensing events of this type will be more frequent as more HPM low mass objects are found in high density environments like the galactic bulge and inner disk, but also with background galaxies. Although the lens candidate we present here is not predicted to pass in front of the center of the galaxy the event can be used to study the lens for unresolved companions and planets. In this case this maybe particularly difficult as the lens goes through different parts of the galaxy in short time scales magnifying regions

of intrinsically different brightness. These events can also be used to make more detailed structural studies of galaxies at low redshift.

## ACKNOWLEDGEMENTS

The authors thank the referee Dr. Nigel Hambly for his comments and suggestions that helped to improve the quality of the paper. J.C.B., D.M., acknowledges support from: PhD Fellowship from CONICYT, Project FONDECYT No. 1130196. D.M and R.A.M acknowledges project support from Basal Center for Astrophysics and Associated Technologies CATA PFB-06. Support for J.C.B, D.M, R.A.M, M.G and R.K is provided by the Ministry of Economy, Development, and Tourism's Millennium Science Initiative through grant IC120009, awarded to The Millennium Institute of Astrophysics, MAS. A.B. Acknowledges financial support from the Proyecto Fondecyt de Iniciación 11140572. Part of this work was completed at the ESO Headquarters, Garching bei München, with support from the ESO Director General's Discretionary Fund program. R.A.M. acknowledges ESO/Chile for hosting him during his sabbatical-leave throughout 2014. MG acknowledges support from Joined Committee ESO and Government of Chile 2014. This research has made use of the SIMBAD database, operated at CDS, Strasbourg, France This publication makes use of data products from, the Two Micron All Sky Survey, which is a joint project of the University of Massachusetts and the Infrared Processing and Analysis Center/California Institute of Technology, funded by NASA and NSF. This publication makes use of data products from the Wide-field Infrared Survey Explorer, which is a joint project of the University of California, Los Angeles, and the Jet Propulsion Laboratory/California Institute of Technology, funded by the National Aeronautics and Space Administration. Based on data from CMC15 Data Access Service at CAB (INTA-CSIC). This research has benefitted from the M, L, T, and Y dwarf compendium housed at DwarfArchives.org This research has benefitted from the SpeX Prism Spectral Libraries, maintained by Adam Burgasser at <http://pono.ucsd.edu/~adam/browndwarfs/spexprism>

## REFERENCES

- Ahn, C. P., Alexandroff, R., Allende Prieto, C., et al. 2012, *ApJS*, 203, 21
- Allard, F., Homeier, D., & Freytag, B. 2012, *Royal Society of London Philosophical Transactions Series A*, 370, 2765
- Allen, P. R., Burgasser, A. J., Faherty, J. K., & Kirkpatrick, J. D. 2012, *AJ*, 144, 62
- Ammons, S. M., Robinson, S. E., Strader, J., et al. 2006, *ApJ*, 638, 1004
- Artigau, É., Radigan, J., Folkes, S., et al. 2010, *ApJ*, 718, L38
- Bayo, A., Rodrigo, C., Barrado Y Navascués, D., et al. 2008, *A&A*, 492, 277
- Beamín, J. C., Minniti, D., Gromadzki, M., et al. 2013, *A&A*, 557, LL8
- Bidelman, W. P. 1985, *ApJS*, 59, 197
- Bonnarel, F., Fernique, P., Bienaymé, O., et al. 2000, *A&AS*, 143, 33
- Boyd, M. R., Winters, J. G., Henry, T. J., et al. 2011, *AJ*, 142, 10

<sup>9</sup> value obtained using the NED cosmological calculator <http://www.astro.ucla.edu/~wright/CosmoCalc.html>

Table 5. Binary/Multiple system investigated in this paper. The columns are: spectral type are from this work and from literature spectra,  $T_{eff}$  is defined based on photometric spectral energy distribution,  $2MASS$  J band magnitude,  $\rho$  the angular separation in arcsec, D is the photometric distance in pc, except for the labeled objects which have parallaxes,  $\mu_{\alpha}\cos(\delta)$  and  $\mu_{\delta}$  are the proper motion in each celestial coordinate.

Star ID	Sp. type (reference)	$T_{eff}$ [K]	$J_{2MASS}$ [mag]	$\rho$ ['']	Dist. [pc]	$\mu_{\alpha}\cos(\delta)$ [mas]	$\mu_{\delta}$ [mas]	remarks
2MASS J06571510-1446173	M4	3300	10.678	43.6	29.1	70	-270	see ** in table 4
2MASS J06571773-1446382	—	3000	12.751	—	$\sim 40$	61 (1)	-268 (1)	
2MASS J08291581-5850305	K7	4200	10.206	88.49	80.3	363 (4)	-81(4)	Halo wide binary
2MASS J08292286-5849209	—	2900	14.550	—	$\sim 110$	355	-73(1)	
2MASS J14040025-5923551	M2.5	3600	10.219	78.05	$24.78^{+5.4}_{-3.7}$	$8.27\pm 5.9$	$-494.5\pm 5.1$	VVV parallax
2MASS J14035016-5923426	M3	3500	10.258	—	$20.4^{+3.4}_{-2.6}$	$11.5\pm 4.6$	$-492.2\pm 4.3$	
2MASS J15480325-5811119	M1.5(1)	3467(7)	8.379	20.7	23.5(1) 33.6(2)	-593 (1)	-250 (1)	$V_{rad}=30.9$ km/s (1)
2MASS J15480441-5810533	M3.5	3400	10.169	—	29.5	-503 (3)	-207 (3)	
2MASS 19103460-4133443	—	3500	9.851	127.78(A-B) 54.99(A-C)	35.9	72 (5)	-738(5)	Triple system
2MASS 19104599-4133407	M4	3300	10.610	147.90(B-C)	22.8 (6) 27.6	91 (5)	-742 (5)	Component B
2MASS 19103359-4132505	—	3100	11.147	—	29.2	68 (5)	-735 (5)	Component C

(1) Hawley et al. (1996), (2) van Altena et al. (1995), (3) Luhman (2014) (4) Kirkpatrick et al. (2014), (5) Deacon et al. (2005), (6) Winters et al. (2015), (7) Houdebine (2010). The values without reference were calculated or derived in this work, the photometric distances have a  $\lesssim 20\%$  error (spectral type and effective temperature uncertainties are the main source of error).

Burgasser, A. J., Cruz, K. L., Cushing, M., et al. 2010, ApJ, 710, 1142  
 Burgasser, A. J., Geballe, T. R., Leggett, S. K., Kirkpatrick, J. D., & Golimowski, D. A. 2006, ApJ, 637, 1067  
 Burgasser, A. J., McElwain, M. W., Kirkpatrick, J. D., et al. 2004, AJ, 127, 2856  
 Buzzoni, B., Delabre, B., Dekker, H., et al. 1984, The Messenger, 38, 9  
 Cushing, M. C., Vacca, W. D., & Rayner, J. T. 2004, PASP, 116, 362  
 Cushing, M. C., Kirkpatrick, J. D., Gelino, C. R., et al. 2011, ApJ, 743, 50  
 Davison, C. L., White, R. J., Henry, T. J., et al. 2015, AJ, 149, 106  
 Dalton, G. B., Caldwell, M., Ward, A. K., et al. 2006, Proc. SPIE, 6269, 62690X  
 Deacon, N. R., Hambly, N. C., & Cooke, J. A. 2005, A&A, 435, 363  
 Deacon, N. R., Hambly, N. C., King, R. R., & McCaughrean, M. J. 2009, MNRAS, 394, 857  
 Deacon, N. R., Liu, M. C., Magnier, E. A., et al. 2014, ApJ, 792, 119  
 Delorme, P., Lagrange, A. M., Chauvin, G., et al. 2012, A&A,

539, A72  
 Dékány, I., Minniti, D., Catelan, M., et al. 2013, ApJ, 776, LL19  
 Dieterich, S. B., Henry, T. J., Golimowski, D. A., Krist, J. E., & Tanner, A. M. 2012, AJ, 144, 64  
 Dupuy, T. J., & Liu, M. C. 2012, ApJS, 201, 19  
 Elliott, P., Bayo, A., Melo, C. H. F., et al. 2014, A&A, 568, A26  
 Emerson, J., & Sutherland, W. 2010, The Messenger, 139, 2  
 Epchtein, N., de Batz, B., Capoani, L., et al. 1997, The Messenger, 87, 27  
 Faherty, J. K., Burgasser, A. J., Cruz, K. L., et al. 2009, AJ, 137, 1  
 Finch, C. T., Henry, T. J., Subasavage, J. P., Jao, W.-C., & Hambly, N. C. 2007, AJ, 133, 2898  
 Finch, C. T., Zacharias, N., Subasavage, J. P., Henry, T. J., & Riedel, A. R. 2014, AJ, 148, 119  
 Fresneau, A., Vaughan, A. E., & Argyle, R. W. 2007, A&A, 469, 1221  
 Gagné, J., Lafrenière, D., Doyon, R., Malo, L., & Artigau, É. 2015, ApJ, 798, 73  
 Giclas, H. L., Burnham, R., & Thomas, N. G. 1971, Flagstaff, Arizona: Lowell Observatory, 1971,  
 Gonzalez, O. A., Rejkuba, M., Minniti, D., et al. 2011, A&A, 534, LL14

- Gizis, J. E. 1997, *AJ*, 113, 806
- Hambly, N. C., Henry, T. J., Subasavage, J. P., Brown, M. A., & Jao, W.-C. 2004, *AJ*, 128, 437
- Hambly, N. C., & Deacon, N. R. 2005, *Astronomische Nachrichten*, 326, 1011
- Hamuy, M., Suntzeff, N. B., Heathcote, S. R., et al. 1994, *PASP*, 106, 566
- Hawley, S. L., Gizis, J. E., & Reid, I. N. 1996, *AJ*, 112, 2799
- Hempel, M., Minniti, D., Dékány, I., et al. 2014, *The Messenger*, 155, 29
- Henry, T. J., Jao, W.-C., Subasavage, J. P., et al. 2006, *AJ*, 132, 2360
- Høg, E., Fabricius, C., Makarov, V. V., et al. 2000, *A&A*, 355, L27
- Houdebine, E. R. 2010, *MNRAS*, 407, 1657
- Ivanov, V. D., Minniti, D., Hempel, M., et al. 2013, *A&A*, 560, AA21
- Ivanov, V. D., Vaisanen, P., Kniazev, A. Y., et al. 2015, *A&A*, 574, A64
- Jao, W.-C., Henry, T. J., Beaulieu, T. D., & Subasavage, J. P. 2008, *AJ*, 136, 840
- Kirkpatrick, J. D., Henry, T. J., & McCarthy, D. W., Jr. 1991, *ApJS*, 77, 417
- Kirkpatrick, J. D., Reid, I. N., Liebert, J., et al. 1999, *ApJ*, 519, 802
- Kirkpatrick, J. D., Looper, D. L., Burgasser, A. J., et al. 2010, *ApJS*, 190, 100
- Kirkpatrick, J. D., Cushing, M. C., Gelino, C. R., et al. 2011, *ApJS*, 197, 19
- Kirkpatrick, J. D., Gelino, C. R., Cushing, M. C., et al. 2012, *ApJ*, 753, 156
- Kirkpatrick, J. D., Schneider, A., Fajardo-Acosta, S., et al. 2014, *ApJ*, 783, 122
- Kordopatis, G., Gilmore, G., Steinmetz, M., et al. 2013, *AJ*, 146, 134
- Lasker, B. M., Lattanzi, M. G., McLean, B. J., et al. 2008, *AJ*, 136, 735
- Lépine, S., & Shara, M. M. 2005, *AJ*, 129, 1483
- Lépine, S. 2005, *AJ*, 130, 1247
- Lépine, S., & Bongiorno, B. 2007, *AJ*, 133, 889
- Lépine, S. 2008, *AJ*, 135, 2177
- Lépine, S., & Gaidos, E. 2011, *AJ*, 142, 138
- Lépine, S., Hilton, E. J., Mann, A. W., et al. 2013, *AJ*, 145, 102
- Lucas, P. W., Tinney, C. G., Burningham, B., et al. 2010, *MNRAS*, 408, L56
- Luhman, K. L., Loutrel, N. P., McCurdy, N. S., et al. 2012, *ApJ*, 760, 152
- Luhman, K. L. 2013, *ApJ*, 767, LL1
- Luhman, K. L. 2014, *ApJ*, 781, 4
- Luhman, K. L., & Sheppard, S. S. 2014, *ApJ*, 787, 126
- Luhman, K. L. 2014, *ApJ*, 786, LL18
- Luyten, W. J. 1979, *New Luyten catalogue of stars with proper motions larger than two tenths of an arcsecond; and first supplement; NLTT. (Minneapolis (1979))*; Label 12 = short description; Label 13 = documentation by Warren; Label 14 = catalogue, Strasbourg version,
- Luyten, W. J. 1979, *Minneapolis: University of Minnesota*, 1979, 2nd ed.,
- Luyten, W. J., & Hughes, H. S. 1980, *Proper Motion Survey, University of Minnesota*, 55, 1
- Mamajek, E. E., Bartlett, J. L., Seifahrt, A., et al. 2013, *AJ*, 146, 154
- Mamajek, E. E., Barenfeld, S. A., Ivanov, V. D., et al. 2015, *ApJ*, 800, L17
- Mason, B. D., Wycoff, G. L., Hartkopf, W. I., Douglass, G. G., & Worley, C. E. 2001, *AJ*, 122, 3466
- Mendez, R. A., & van Altena, W. F. 1996, *AJ*, 112, 655
- Minniti, D., Lucas, P. W., Emerson, J. P., et al. 2010, *New Astron.*, 15, 433
- Minniti, D., Saito, R. K., Gonzalez, O. A., et al. 2014, *A&A*, 571, AA91
- Monet, D. G., Levine, S. E., Canzian, B., et al. 2003, *AJ*, 125, 984
- Muñoz, J. L., & Evans, D. W. 2014, *Astronomische Nachrichten*, 335, 367
- Pecaut, M. J., & Mamajek, E. E. 2013, *ApJS*, 208, 9
- Pickles, A. J. 1998, *PASP*, 110, 863
- Pickles, A., & Depagne, É. 2010, *PASP*, 122, 1437
- Salim, S., & Gould, A. 2003, *ApJ*, 582, 1011
- Saito, R. K., Hempel, M., Minniti, D., et al. 2012, *A&A*, 537, A107
- Simcoe, R. A., Burgasser, A. J., Schechter, P. L., et al. 2013, *PASP*, 125, 270
- Simcoe, R. A., et al. 2010, *Proc. SPIE*, 7735,
- Simcoe, R. A., Burgasser, A. J., Bernstein, R. A., et al. 2008, *Proc. SPIE*, 7014, 70140U
- Scholz, R.-D. 2014, *A&A*, 561, A113
- Skrutskie, M. F., et al. 2006, *AJ*, 131, 1163
- Smart, R. L., Lattanzi, M. G., Bucciarelli, B., et al. 2003, *A&A*, 404, 317
- Smith, L., Lucas, P. W., Burningham, B., et al. 2014, *MNRAS*, 437, 3603
- Snodgrass, C., Saviane, I., Monaco, L., & Sinclaire, P. 2008, *The Messenger*, 132, 18
- Subasavage, J. P., Henry, T. J., Hambly, N. C., Brown, M. A., & Jao, W.-C. 2005, *AJ*, 129, 413
- Subasavage, J. P., Henry, T. J., Hambly, N. C., et al. 2005, *AJ*, 130, 1658
- Taylor, M. B. 2005, *Astronomical Data Analysis Software and Systems XIV*, 347, 29
- Vacca, W. D., Cushing, M. C., & Rayner, J. T. 2003, *PASP*, 115, 389
- van Altena, W. F., Lee, J. T., & Hoffleit, E. D. 1995, *New Haven, CT: Yale University Observatory, |c1995, 4th ed., completely revised and enlarge*
- Wenger, M., Ochsenbein, F., Egret, D., et al. 2000, *A&AS*, 143, 9
- Winters, J. G., Hambly, N. C., Jao, W.-C., et al. 2015, *AJ*, 149, 5
- Wright, E. L., Eisenhardt, P. R. M., & Mainzer, A. K. et al. 2010, *AJ*, 140, 1868
- Wright, E. L., Mainzer, A., Kirkpatrick, J. D., et al. 2014, *AJ*, 148, 82
- Wroblewski, H., & Torres, C. 1989, *A&AS*, 78, 231
- Zacharias, N., Finch, C. T., Girard, T. M., et al. 2013, *AJ*, 145, 44

This paper has been typeset from a  $\text{\TeX}/\text{\LaTeX}$  file prepared by the author.